35th AIAA Fluid Dynamics Conference, June 6–9, 2005/Toronto,Canada

Preliminary Study of the Turbulence Structure in Supersonic Boundary Layers using DNS Data

Ellen M. Taylor*, M. Pino Martín† and Alexander J. Smits‡
Mechanical and Aerospace Engineering Department
Princeton University, Princeton, NJ

Direct numerical simulation data are used to visualize coherent structures in turbulent boundary layers at Mach numbers from 0.3 to 7. Different criteria to identify the three-dimensional turbulence structure are selected. We find that using the discriminant of the velocity gradient tensor, the swirling strength and the λ_2 criteria give nearly identical results, with λ_2 identifying more structures very close to the wall.

I. Introduction

Recent direct numerical simulations (DNS) provide a detailed database[1] of turbulent boundary layers over a wide range of freestream and wall-temperature conditions. In this paper, we use the DNS database to further assess the structure of turbulent boundary layers in the inner and outer layers.

About 75% of the total production of turbulent kinetic energy occurs in the range of $z/\delta = 0.2$, where z is the wall-normal direction and δ is the boundary layer thickness. Previous work[2,3,4] has shown that the viscous sublayer in a boundary layer is occupied by alternating streaks of high- and low-speed fluid. The spanwise spacing of the streaks is found to scale on inner variables and to have a mean value of $\lambda_s \approx 100$. This result is independent of the Reynolds number over the range of $740 < Re_\theta < 5,830$.[5] The streaks are assumed to be a result of elongated, counter-rotating streamwise vortices that appear near the wall. Kline *et al.*[3] observe that the low-speed streaks gradually lift up from the wall, oscillate, and then break up violently, ejecting fluid away from the wall and into the outer layer. This sequence of events is known as "bursting." Kim *et al.*[6] found that in $0 < z^+ < 100$ most of the turbulence production occurs during bursting events, indicating the significant importance of the near-wall region and the bursting process. The scaling of the bursting frequency, however, is still controversial. It is not clear whether an inner or an outer scaling is appropriate. In addition, there does not exist a unified criteria for identifying the bursting event.

For moderate Mach numbers, the outer region (beyond the logarithmic region) is dominated by the entrainment process rather than by turbulence production. The characteristic structure of the outer layer is the large-scale turbulent "bulge", also known as large-scale motion (LSM). These structures evolve and decay slowly and are inclined to the wall at an acute angle, leaning in the downstream direction. The characteristic properties of the LSM, such as length scale, time scale, convection velocity, and structure angle, as well as their internal structure, such as velocity, vorticity and pressure fields, remain the subject of active research.

In this paper, we present a study of the structure parameter and the visualization of coherent, organized motions for turbulent boundary layers in the Mach number range from 0.3 to 7.

*Student member
†AIAA Member pmartin@princeton.edu
‡AIAA Fellow

Case	M_δ	ρ_δ (kg/m^3)	T_δ (K)	T_w/T_δ	Re_θ	θ (mm)	H	δ (mm)
MI	0.30	1.0000	300.00	1.00	1618	0.287	1.4	2.56
M3	2.98	0.0907	219.55	2.58	2390	0.430	5.4	6.04
M5	4.97	0.0937	220.97	5.40	6225	0.657	12.2	14.82
M7	6.95	0.0963	221.61	9.60	10160	0.778	22.3	28.60

Table 1. Dimensional boundary layer edge and wall parameters for the DNS database.

II. DNS flow conditions and resolution

We perform parametric studies with varying freestream Mach number. For the supersonic calculations, the freestream conditions are atmospheric at 20 km altitude. The Mach 0.3 simulation is at sea level. The Reynolds numbers for the mean flow profiles are based on the maximum values for which we can gather DNS statistics in a reasonable number of days. With this criterion, we compute a typical DNS simulation in roughly three days using 45% of the current computational resources in the CROCCO Laboratory at Princeton University. The number of grid points required for accurate DNS depends on $\delta^+ = \delta/z_\tau$, where δ is the boundary layer thickness and z_τ is the wall unit. For the current simulations δ^+ is about 350, so that the Reynolds number based on the momentum thickness, Re_θ, increases with Mach number. It should be noted that, in the near-wall region, the Reynolds number dependence is removed when plotting the data in wall units.

Table 1 lists the boundary-layer-edge and wall-temperature conditions for the DNS calculations, as well as Re_θ, δ and relevant integral parameters. We use isothermal wall-conditions for all calculations with wall temperature, T_w, prescribed to the nearly adiabatic temperature. We use freestream Mach numbers in the range of 0.3 to 7. Table 2 lists the grid resolution and domain size for the same simulations. We gather statistics for one non-dimensional time unit, which corresponds to about 75 δ^*/U_δ units, where δ^* is the displacement thickness and U_δ is the mean velocity at the boundary layer edge.

III. Accuracy of the DNS data

Details about the numerical method and the assessment of the DNS data are given in Martin.[1] Here, we briefly comment on the accuracy of the data. Figure 1 plots the van-Driest transformed velocity profiles for the DNS data. There is good agreement between the theory and the numerical data. Figure 2 plots the skin friction coefficient given by the DNS data in comparison to the theoretical predictions.[7] The error bars show an 8% departure from the theory.

Case	δ^+	L_x/δ	L_y/δ	L_z/δ	Δx^+	Δy^+	N_x	N_y	N_z
MI	583	5.6	1.4	16.6	8.5	3.2	384	256	116
M3	325	9.1	2.3	13.8	8.0	3.0	384	256	106
M5	382	7.4	1.8	14.0	7.4	2.8	384	256	110
M7	414	6.4	1.6	14.8	7.0	2.6	384	256	112

Table 2. Grid resolution and domain size for the direct numerical simulations.

IV. Structure Identification Criteria

The identification of coherent structures is not trivial. It is not clear that vorticity alone is a good criterion because it may change drastically across a typical structure. For example, in hairpin structures, the vorticity changes across a shear layer as well as from the exterior of a vortex core to its interior. In order to clearly isolate structures while minimizing noise, we require quantitative measures that more closely reflect our intuitive recognition of a coherent structure.

Before describing a selection of parameters for identifying structures, we provide some definitions. If A is a general real 3×3 matrix, its characteristic equation is

$$\lambda^3 + P\lambda^2 + Q\lambda + R = 0 \tag{1}$$

in which $P = -\mathrm{tr}\,(A)$, $Q = \frac{1}{2}\left[P^2 - \mathrm{tr}\,(AA)\right]$, and $R = \frac{1}{3}\left[-P^3 + 3PQ - \mathrm{tr}\,(AAA)\right]$. The definition $\lambda = \tilde{\lambda} - \frac{1}{3}P$ allows Eqn. (1) to be reduced to

$$\tilde{\lambda}^3 + \tilde{Q}\tilde{\lambda} + \tilde{R} = 0 \tag{2}$$

in which $\tilde{Q} = Q - \frac{1}{3}P^2$ and $\tilde{R} = R + \frac{2}{27}P^3 - \frac{1}{3}PQ$. A crucial indicator of the qualitative character of the eigenvalues of A is the discriminant

$$\Delta = \left(\tfrac{1}{3}\tilde{Q}\right)^3 + \left(\tfrac{1}{2}\tilde{R}\right)^2 \tag{3}$$

When $\Delta > 0$, there exists one real eigenvalue and one complex conjugate pair of eigenvalues, and when $\Delta \leq 0$, all three eigenvalues are real. No other arrangement is possible.

A. Fluid Velocity Gradient Tensor

Consider the case

$$A_{ij} = \frac{\partial u_i}{\partial x_j} \tag{4}$$

in which u_i is the ith component of the velocity vector. To linear order $u_i\,(x_j + \delta x_j) = u_i\,(x_j) + A_{ij}\,\delta x_j$. Thus the eigenvalues of A_{ij} characterize a fluid's local velocity field. Chong *et al.*[8] noted that the complex conjugate pair in regions where $\Delta > 0$ indicates a spiraling motion consistent with the presence of vortices. Therefore, monitoring the positive values of the discriminant of the velocity gradient tensor is one method for recognizing coherent structures.

Zhou *et al.*[9] agreed with the fundamental logic of Chong *et al.*[8] but preferred to gather the numerical quantity of interest from the eigenvalues themselves. If we define λ_{ci} as the imaginary part of one of the

complex pairs, then

$$\lambda_{ci}^2 = \frac{3}{4}\left[\left(\tfrac{1}{2}\tilde{R} + \sqrt{\Delta}\right)^{\frac{1}{3}} - \left(\tfrac{1}{2}\tilde{R} - \sqrt{\Delta}\right)^{\frac{1}{3}}\right]^2 \tag{5}$$

This is known in their paper as the swirling strength. As with Δ, λ_{ci}^2 is forced to be zero wherever $\Delta < 0$. Christensen and Adrian[10] have successfully employed this second structure identification measure in turbulent channel flow.

B. Hessian of Pressure

In addition to a spiraling velocity pattern, a vortex core exhibits a local pressure minimum that extends along its length. The analysis here follows that of Jeong and Hussain[11] for incompressible flow. With the definitions $S_{ij} = \frac{1}{2}\left(\frac{\partial u_i}{\partial x_j} + \frac{\partial u_j}{\partial x_i}\right)$ and $\Omega_{ij} = \frac{1}{2}\left(\frac{\partial u_i}{\partial x_j} - \frac{\partial u_j}{\partial x_i}\right)$, the incompressible Navier-Stokes equations become

$$\frac{Du_i}{Dt} = -\frac{1}{\rho}\frac{\partial p}{\partial x_i} + 2\nu\frac{\partial S_{ik}}{\partial x_k} \tag{6}$$

Applying a gradient and isolating its symmetric component, we find that

$$\frac{DS_{ij}}{Dt} + S_{ik}S_{jk} + \Omega_{ik}\Omega_{kj} = -\frac{1}{\rho}\frac{\partial^2 p}{\partial x_i \partial x_j} + \nu\frac{\partial^2 S_{ij}}{\partial x_k^2} \tag{7}$$

We refer to the operator $\frac{\partial^2}{\partial x_i \partial x_j}$ as the Hessian. Within a vortex core, irrotational strain and viscous effects are negligible so that equation (7) reduces to

$$S_{ik}S_{jk} + \Omega_{ik}\Omega_{kj} = -\frac{1}{\rho}\frac{\partial^2 p}{\partial x_i \partial x_j} \tag{8}$$

Because the Hessian of pressure is symmetric, each of its eigenvalues must be real. If at least two of those are furthermore positive, a pressure minimum exists in some two-dimensional cross-section and suggests the presence of a vortex. From equation (8) this condition is satisfied if at least two eigenvalues of $S_{ik}S_{jk}+\Omega_{ik}\Omega_{kj}$ are negative. Note that this matrix is also symmetric by construction. Set

$$A_{ij} = S_{ik}S_{jk} + \Omega_{ik}\Omega_{kj} \tag{9}$$

Using $\theta = \cos^{-1}\left[\frac{1}{2}\tilde{R}\cdot(-\frac{1}{3}\tilde{Q})^{-\frac{3}{2}}\right]$,

$$\tilde{\lambda} = 2\left(-\tfrac{1}{3}\tilde{Q}\right)^{\frac{1}{2}}\cos\left(\frac{\theta + 2n\pi}{3}\right) \tag{10}$$

in which $n \in \{0, 1, 2\}$. If we order the final eigenvalues such that

$$\lambda_1 \leq \lambda_2 \leq \lambda_3 \tag{11}$$

then $\lambda_2 < 0$ is a necessary and sufficient condition for the existence at least two negative eigenvalues of A. Paralleling our treatment of the previous two structure identification criteria, we set λ_2 to be zero wherever $\lambda_2 > 0$ and switch its sign elsewhere.

In summary, we select three possible structure-identification criteria: the discriminant of the velocity gradient tensor Δ, the swirling strength λ_{ci}^2, and λ_2. While the first two are valid for compressible as well as incompressible flows, the current derivation of the third assumes incompressibility.

V. Flow fields from instantaneous DNS Data

In this section, we present the visualization of the turbulence structures for the DNS data of turbulent boundary layers in the Mach number range of 0.3 to 7.

Figure 3 plots contours of spanwise vorticity and velocity vectors on streamwise-wall-normal planes for the Mach 0.3 case. A constant convection speed of $0.75U_\infty$ has been subtracted from the u components of the velocity vector to highlight the vortical motion. We observe the hairpin structures. The heads are identified by the concentric swirling vectors and the tails by the shear-layers that connect the heads to the wall. Six of these structures are identified in this instantaneous flow field. The heavy line marks a single contour of the discriminant of the velocity gradient tensor. Note that the contour of the discriminant is aligned with the hairpin heads, thus indicating the location of the hairpins.

For supersonic flows, we look at simultaneous contours of vorticity and pressure. Thus, regions of high vorticity and low pressure serve to identify hairpin cores. Figures 4 through 6 plot contours of spanwise vorticity and pressure with imposed velocity vectors on streamwise-wall-normal planes for Mach 3 through 7. The relative motion of the turbulence structures has been subtracted and the heavy line indicates a single contour of the discriminant of the velocity gradient tensor. Consistently for all Mach numbers, we find that regions of high vorticity are correlated with regions of low pressure, where hairpins are found. It should be noted that vorticity alone is ambiguous. The hairpin heads are identified by the concentric swirling vectors and the hairpin tails are identified by the shear-layers. The contour of the discriminant overlaps with the hairpin heads for all Mach numbers.

Figure 7 plots iso-surfaces of the various structure-identification parameters for the Mach 0.3 case. The iso-surface values are selected so that the volume of data is not over-populated with structures and structures are clearly identified. All quantities, discriminant of the velocity gradient tensor, swirling strength and λ_2, give similar results for this case. There is a small difference when using the λ_2 criteria. Namely, more near-wall structures are identified with this quantity.

Figures 8 through 10 plot the various structure-identification parameters for the Mach 3 through 7 data. Consistently, all quantities give similar representations of the turbulence structures. As it is found in the incompressible case, the λ_2 criteria identifies more structures near the wall.

Figure 11 plots contours of velocity on streamwise-spanwise planes at $z^+ = 15$ for all cases. The streaky structures are apparent and extend between 100 and 80 wall units apart along the spanwise direction for the Mach 0.3 to Mach 7 data. The heavy line is a single contour of λ_2. We observe no correlation between the streaks and the λ_2 structure identification criteria.

VI. Conclusion

In this paper, we present a preliminary study of the turbulence structure in supersonic turbulent boundary layers from DNS data. Using simultaneous contours of vorticity and pressure, we identify regions that are characteristic of the presence of hairpin structures even at Mach 7 conditions. We also find that vorticity contours alone are not sufficient for identifying turbulence structures. Various structure-identification criteria are used to visualize the three-dimensional hairpin structures, namely: the discriminant of the velocity gradient tensor, the swirling strength, and the λ_2 criteria. We find that all criteria give nearly identical representation of the structures, with the slight difference of the λ_2 criteria, which identifies more structures in the near-wall region. We find, however, that none of the structure-identification criteria serve to identify the streaks in the viscous sublayer. These data are preliminary, and multiple instantaneous samples are required to provide a quantitative study of the turbulence structure in supersonic boundary layers.

VII. Acknowledgments

This work was supported by NSF Grant # CTS-0238390.

References

[1]Martin, M., "DNS of Hypersonic Turbulent Boundary Layers," *AIAA Paper No. 2004-2337*, 2004.

[2]Runstadler, P., Kline, S., and Reynolds, W., "An experimental investigation of flow structure of the turbulent boundary layer," *Mechanical Engineering Department, Stanford University Report MD-8*, 1963.

[3]Kline, S., Reynolds, W., Schraub, F., and Runstadler, P., "The structure of turbulent boundary layers," *Journal of Fluid Mechanics*, Vol. 30, 1967, pp. 741–773.

[4]Bakewell, H. and Lumley, J., "Viscous sublayer and adjacent wall region in turbulent pipe flow," *Physics of Fluids*, Vol. 10, 1967.

[5]Smith, D. and Metzler, S., "The characteristics of low-speed streaks in the near-wall region of a turbulent boundary layer," *Journal of Fluid Mechanics*, Vol. 129, 1983, pp. 27–54.

[6]Kim, H., Kline, S., and Reynolds, W., "The production of turbulence near a smooth wall in a turbulent boundary layer," *Journal of Fluid Mechanics*, Vol. 50, 1971, pp. 133–160.

[7]Van-Driest, E., "Problem of aerodynamic heating," *Aeronautical Engineering Review*, Vol. 15, 1956, pp. 26–41.

[8]Chong, M. S., Perry, A. E., and Cantwell, B. J., "A general classification of three-dimensional flow fields," *Physics of Fluids A*, Vol. 2, No. 5, 1999, pp. 765–777.

[9]Zhou, J., Adrian, R. J., Balachandar, S., and Kendall, T. M., "Mechanisms for generating coherent packets of hairpin vortices in channel flow," *Journal of Fluid Mechanics*, Vol. 387, 1999, pp. 353–396.

[10]Christensen, K. T. and Adrian, R. J., "Statistical evidence of hairpin vortex packets in wall turbulence," *Journal of Fluid Mechanics*, Vol. 431, 2001, pp. 433–443.

[11]Jeong, J. and Hussain, F., "On the identification of a vortex," *Journal of Fluid Mechanics*, Vol. 285, 1995, pp. 69–94.

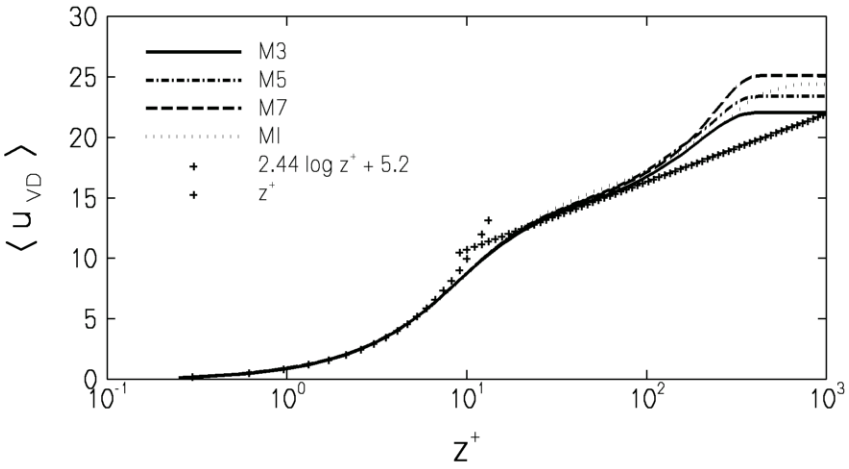

(a)

Figure 1. Mean velocity profiles for the DNS database.

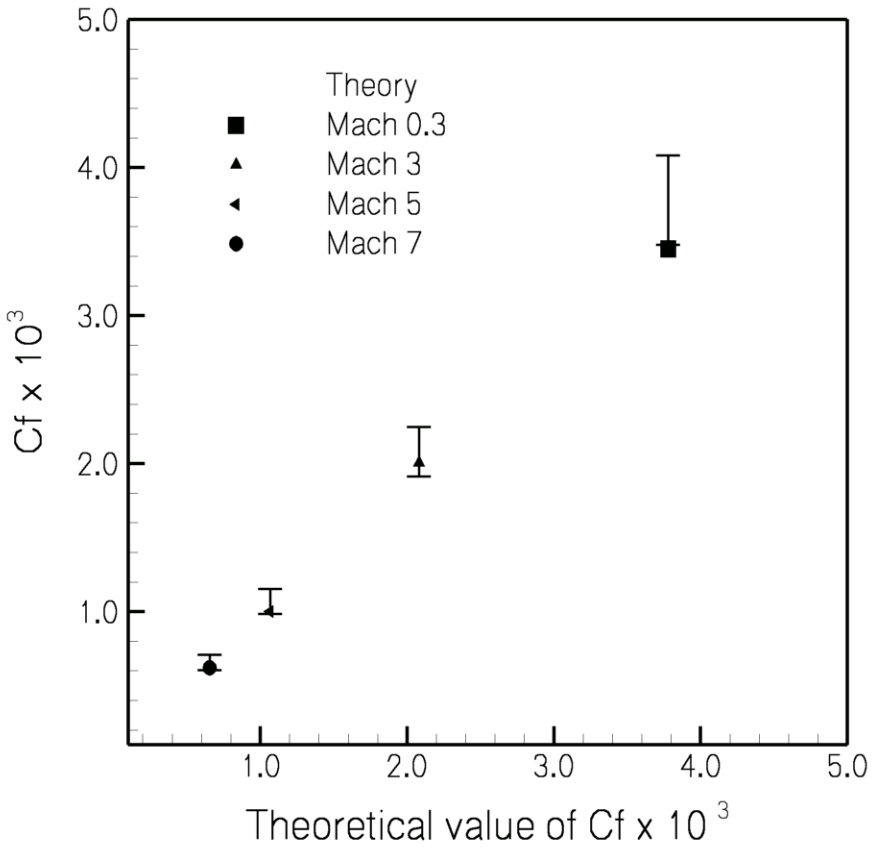

(a)

Figure 2. Skin friction coefficients for the DNS.

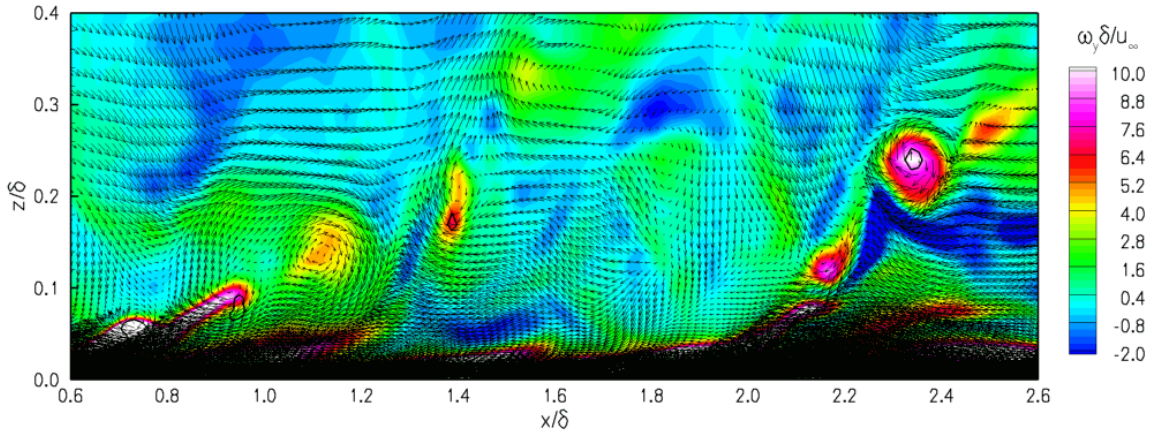

(a)

Figure 3. Streamwise/wall-normal plane of a Mach 0.3 turbulent boundary layer. The heavy line marks a single contour of the discriminant of the velocity gradient tensor, and colored contours represent vorticity. A constant speed of $0.75U_\infty$ has been subtracted from the u components of the velocity vector to highlight vortical motion.

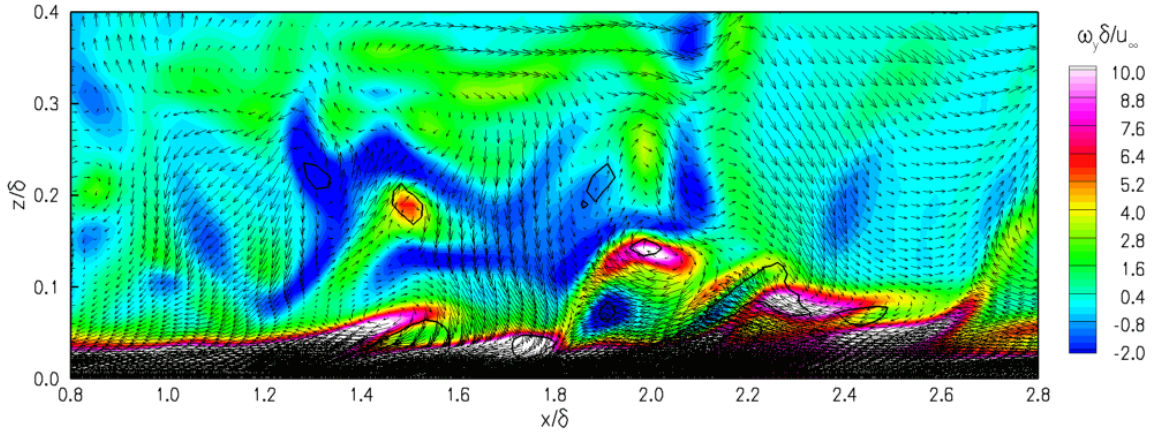

(a) Vorticity contours

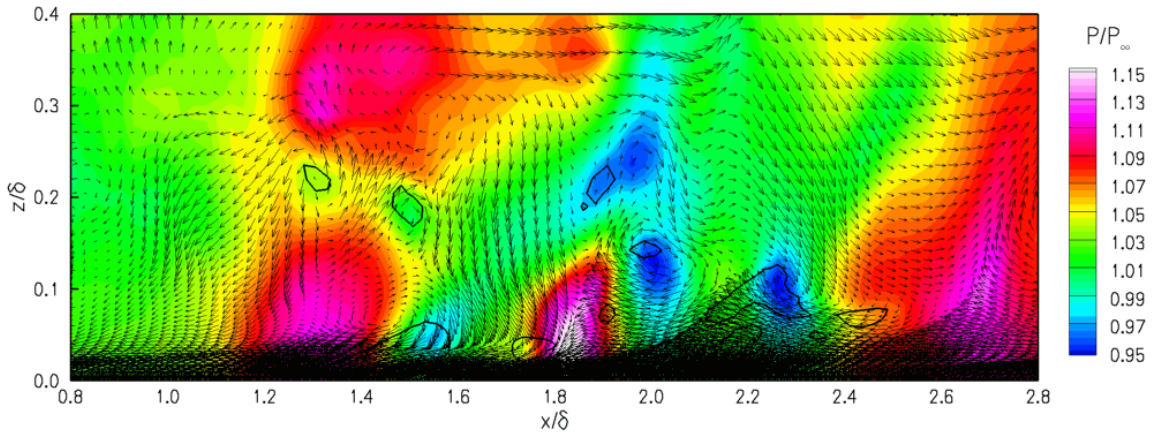

(b) Pressure contours

Figure 4. Streamwise/wall-normal plane of a Mach 3 turbulent boundary layer. The heavy line marks a single contour of the discriminant of the velocity gradient tensor, and colored contours represent the different quantities in each subfigure. A constant speed of $0.75U_\infty$ has been subtracted from the u components of the velocity vector to highlight vortical motion.

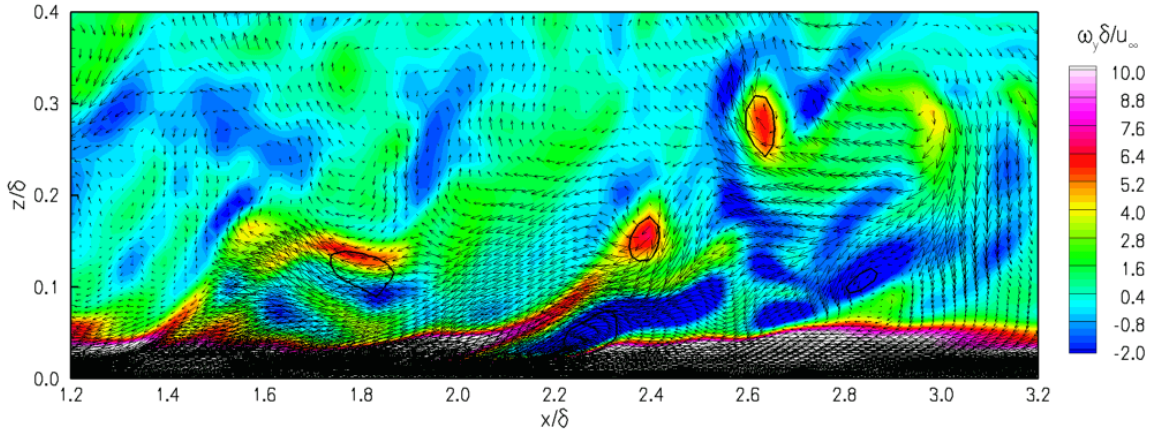

(a) Vorticity contours

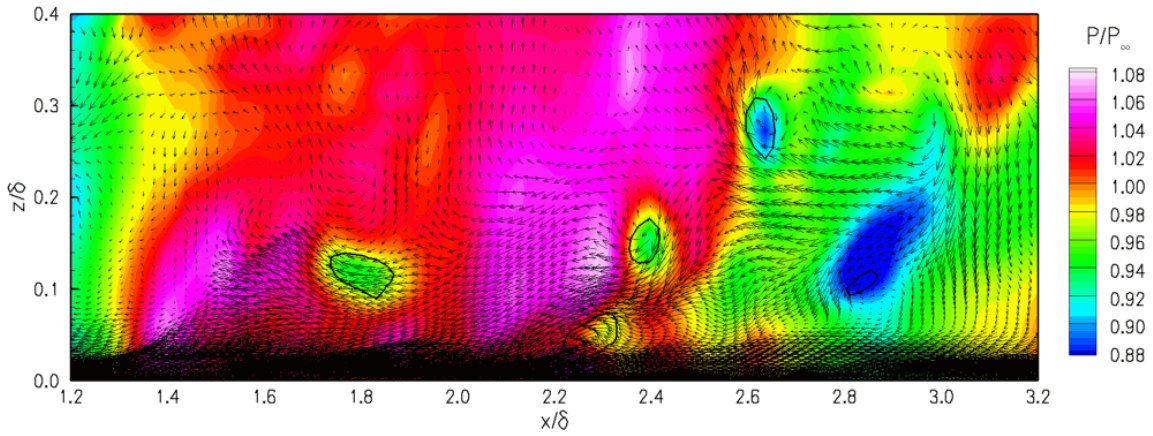

(b) Pressure contours

Figure 5. Streamwise/wall-normal plane of a Mach 5 turbulent boundary layer. The heavy line marks a single contour of the discriminant of the velocity gradient tensor, and colored contours represent the different quantities in each subfigure. A constant speed of $0.7U_\infty$ has been subtracted from the u components of the velocity vector to highlight vortical motion.

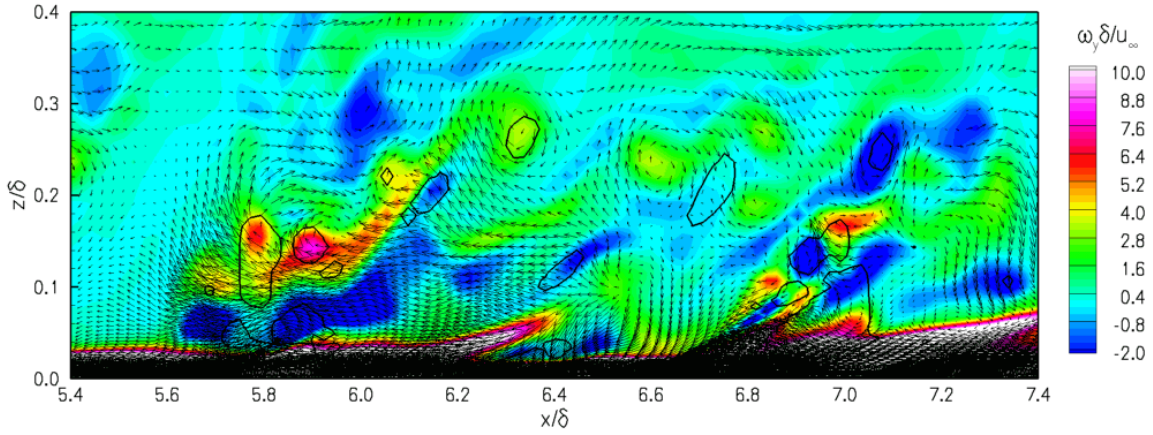

(a) Vorticity contours

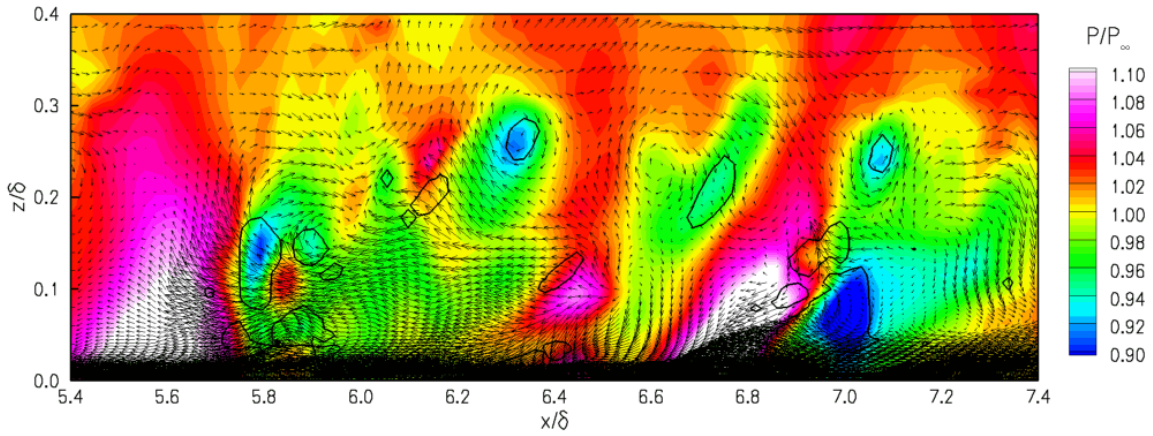

(b) Pressure contours

Figure 6. Streamwise/wall-normal plane of a Mach 7 turbulent boundary layer. The heavy line marks a single contour of the discriminant of the velocity gradient tensor, and colored contours represent the different quantities in each subfigure. A constant speed of $0.75U_\infty$ has been subtracted from the u components of the velocity vector to highlight vortical motion.

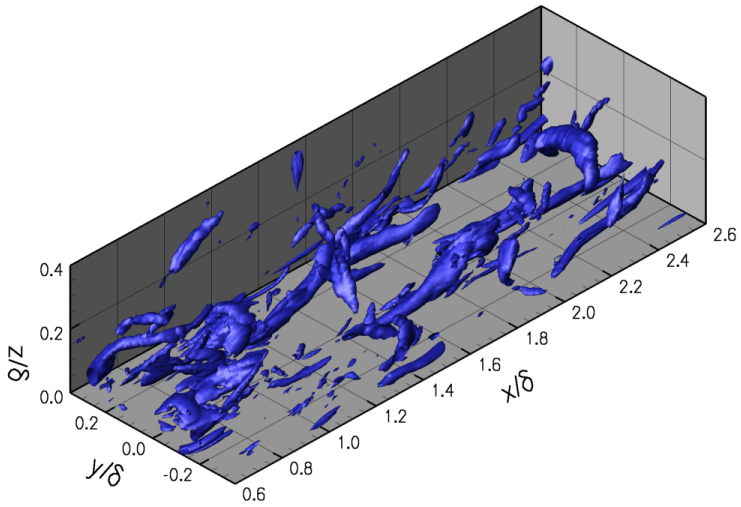

(a) Δ: 2 $\times 10^{-5}$ of the maximum value.

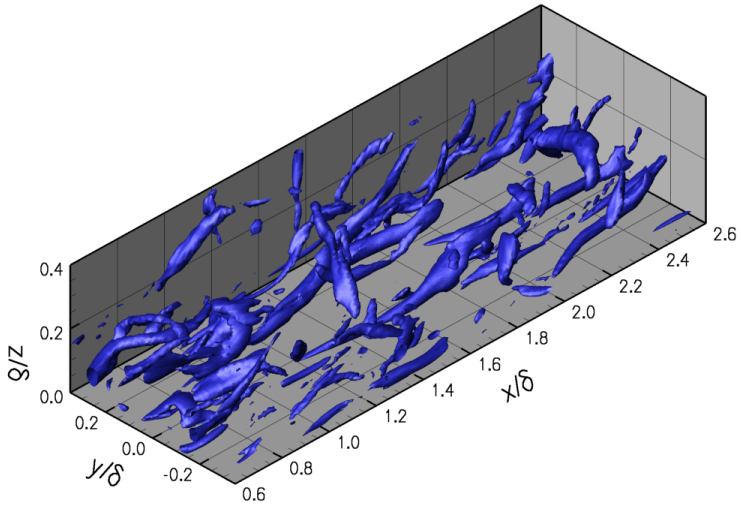

(b) λ_{ci}^2: 0.02 of the maximum value.

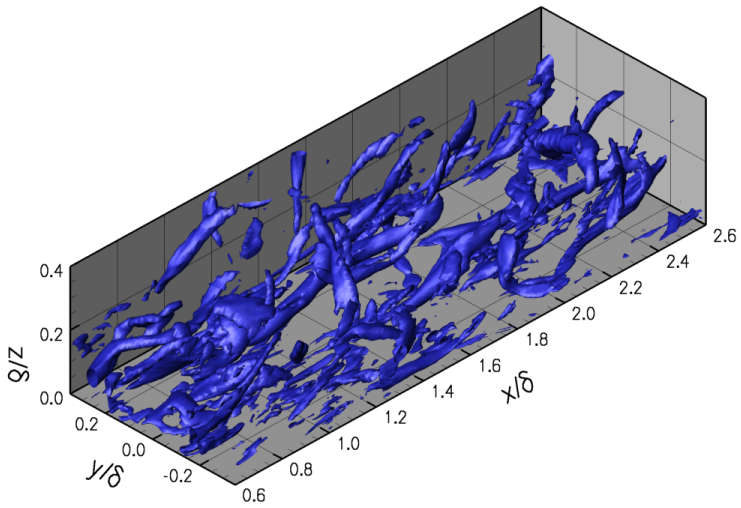

(c) λ_2: 0.02 of the maximum value.

Figure 7. Iso-surfaces of various structure-identification parameters in a Mach 0.3 turbulent boundary layer

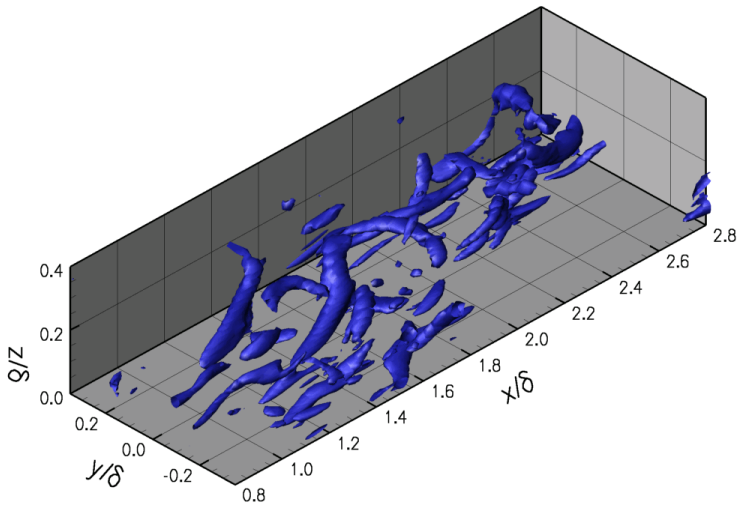

(a) Δ: 2 $\times 10^{-4}$ of the maximum value.

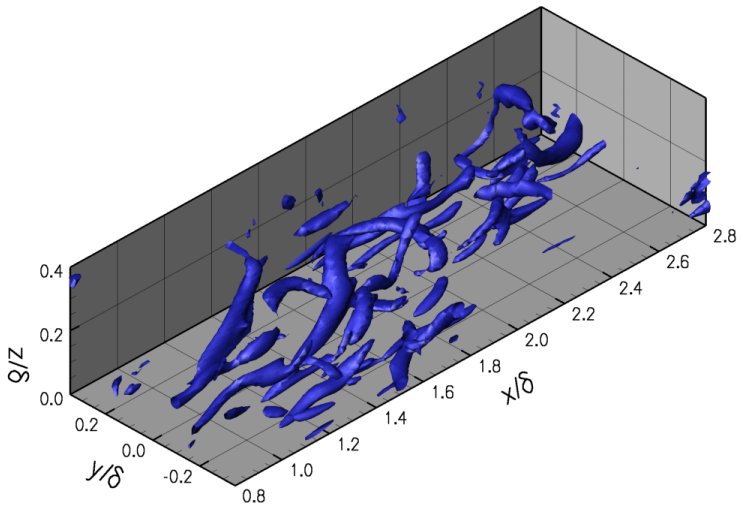

(b) λ_{ci}^2: 0.05 of the maximum value.

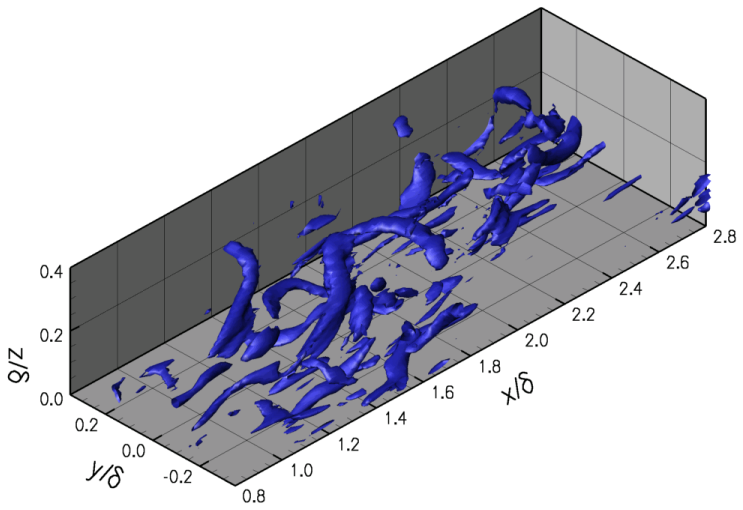

(c) λ_2: 0.05 of the maximum value.

Figure 8. Iso-surfaces of various structure-identification parameters in a Mach 3 turbulent boundary layer

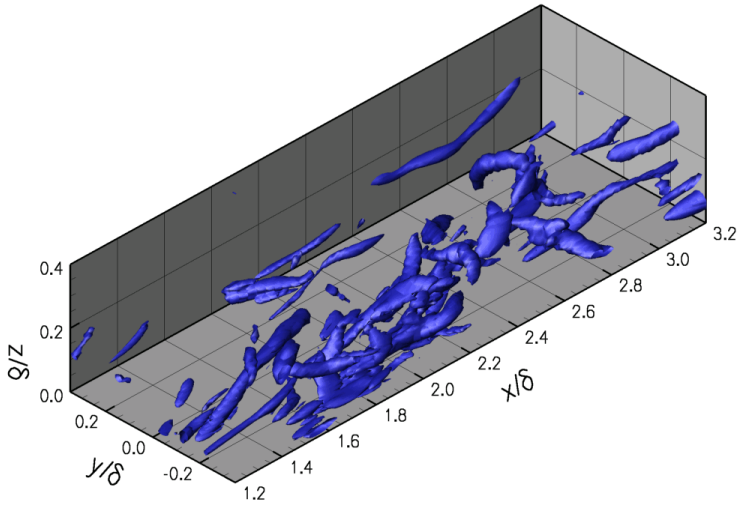

(a) Δ: 2 $\times 10^{-4}$ of the maximum value.

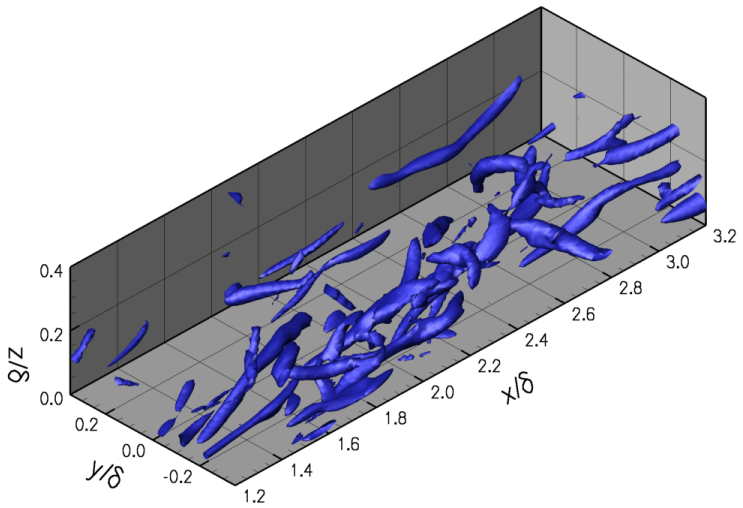

(b) λ_{ci}^2: 0.05 of the maximum value.

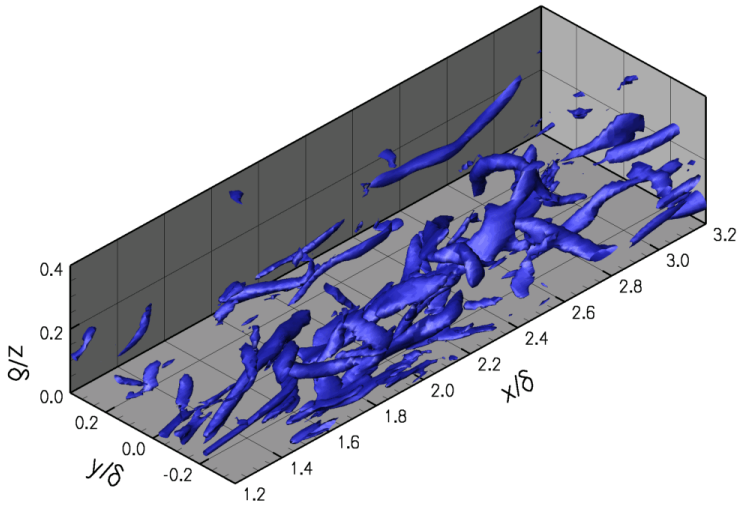

(c) λ_2: 0.05 of the maximum value.

Figure 9. Iso-surfaces of various structure-identification parameters in a Mach 5 turbulent boundary layer

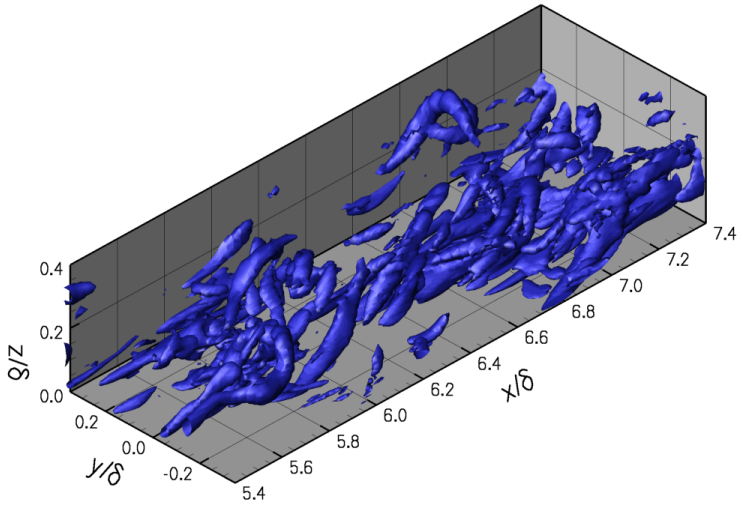

(a) Δ: 2 $\times 10^{-4}$ of the maximum value.

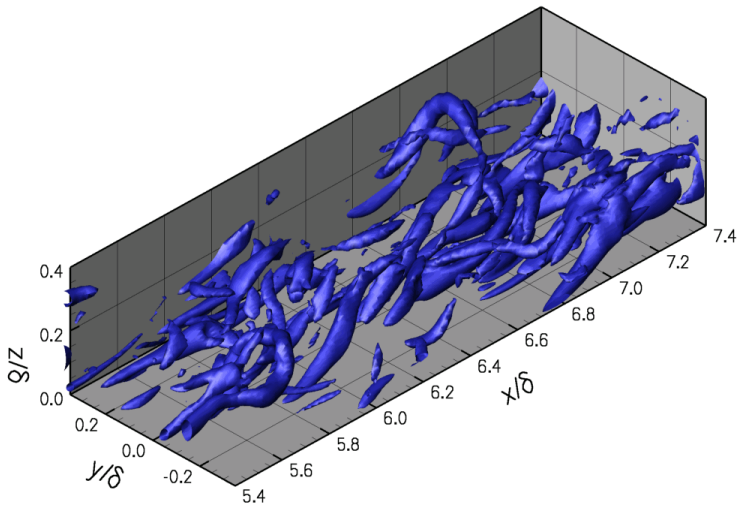

(b) λ_{ci}^2: 0.05 of the maximum value.

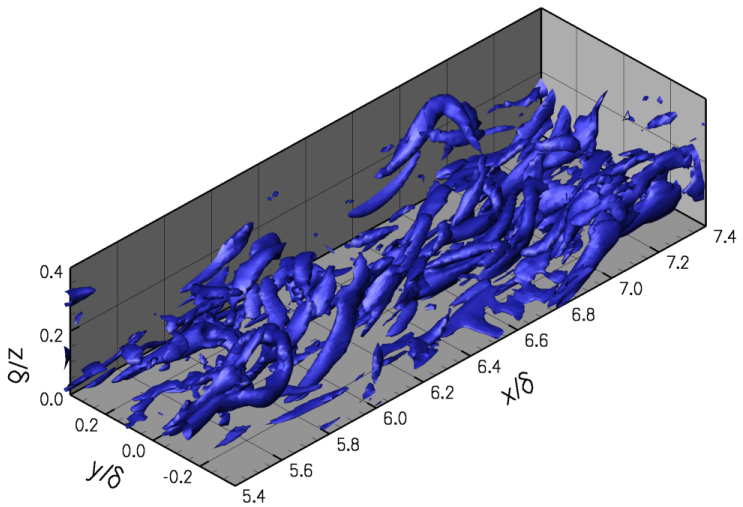

(c) λ_2: 0.05 of the maximum value.

Figure 10. Iso-surfaces of various structure-identification parameters in a Mach 7 turbulent boundary layer

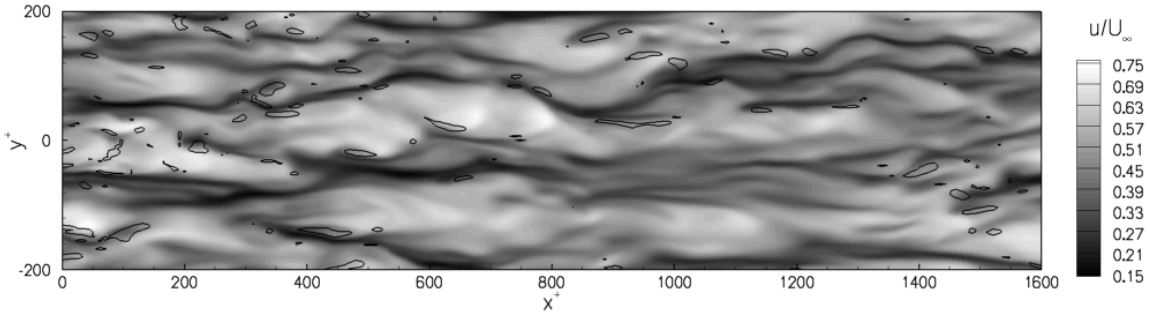

(a) Mach 0.3

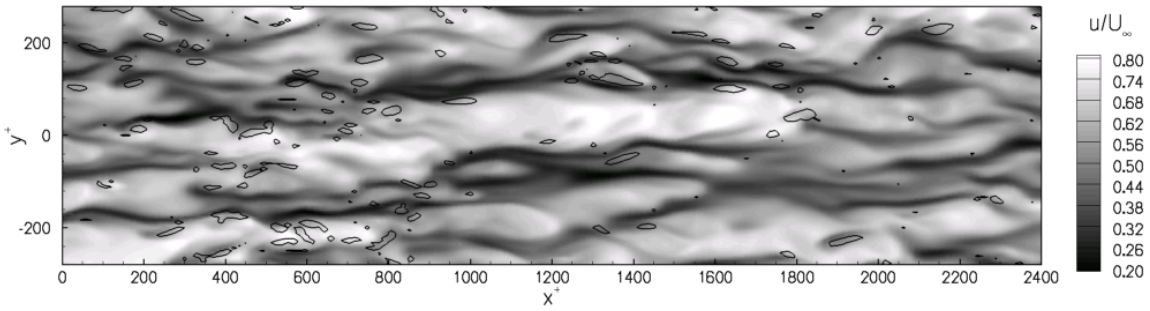

(b) Mach 3

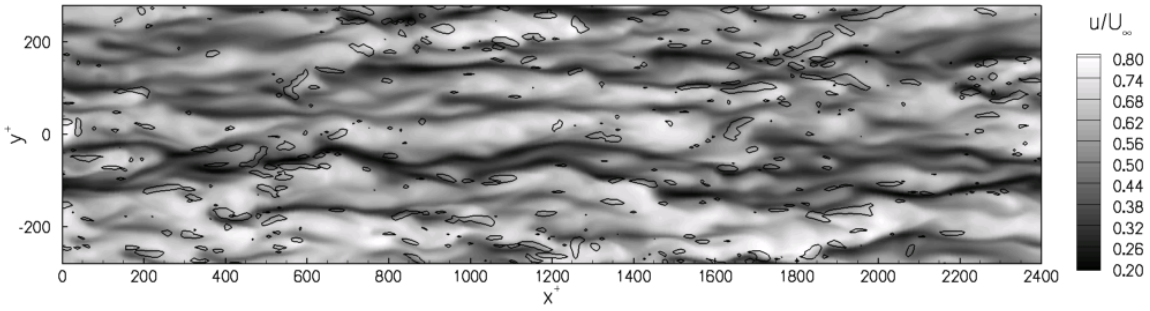

(c) Mach 5

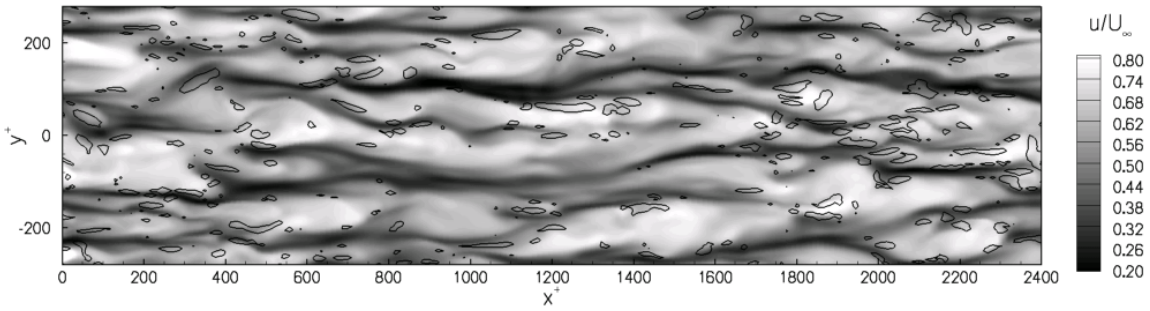

(d) Mach 7

Figure 11. Streamwise/spanwise planes at $z^+ \approx 15$ in turbulent boundary layers of varying freestream Mach numbers. Colored contours show streamwise velocity, and the heavy line is a single contour of λ_2.

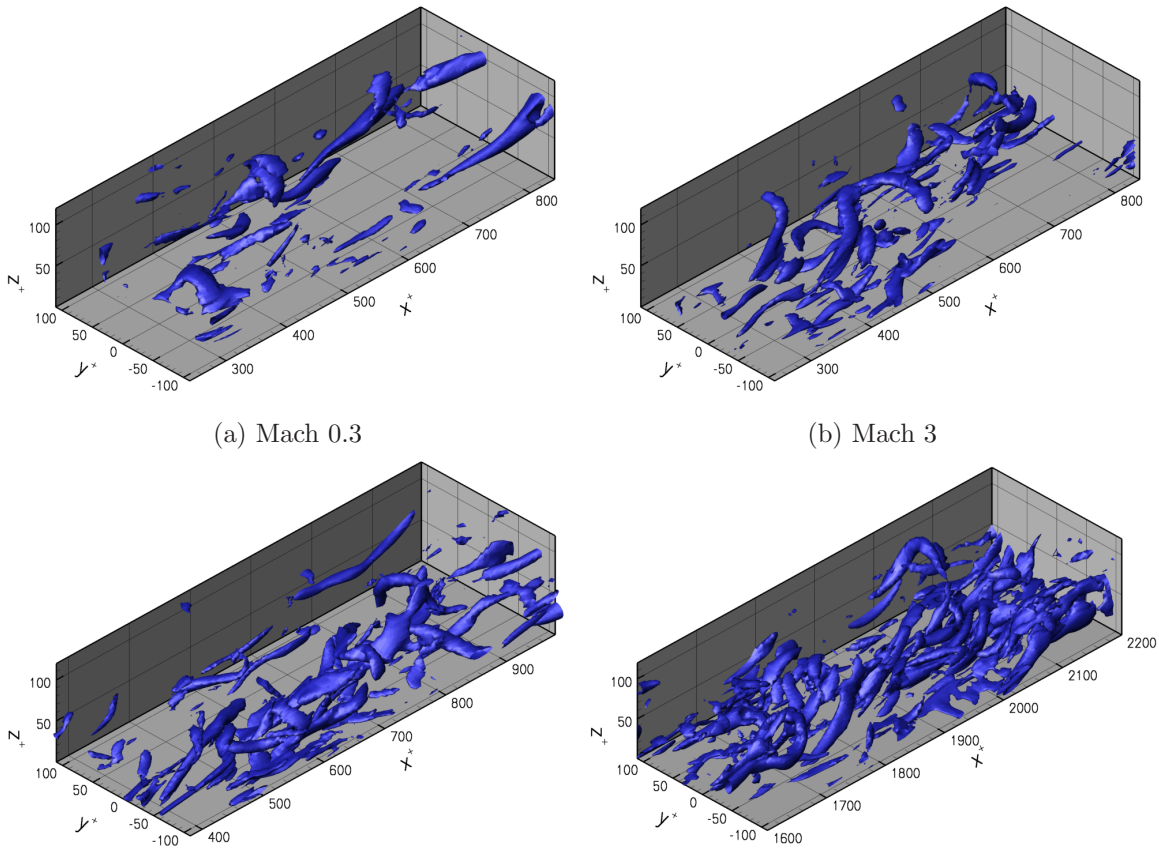

(a) Mach 0.3

(b) Mach 3

(c) Mach 5

(d) Mach 7

Figure 12. Iso-surfaces of λ_2 (0.05 of the maximum value) in wall-unit coordinates for turbulent boundary layers at the various Mach numbers.